CASE STUDY

Vacuum-PVD Improvement: a Case Study of the Second Improvement of Soft Bangkok Clay on the Subsiding Ground

Dennes T. Bergado[1] · Pitthaya Jamsawang[2] · Nuttapong Kovittayanon[3] · Francisco Baez[4] · Peter Tijl de Zwart[4]

Abstract

This paper describes a case study of the second improvement of soft Bangkok clay utilizing a vacuum-PVD combined with embankment preloading. Airtight membranes, horizontal prefabricated drains, and field-distributed air–water separation vacuum systems were applied in this case study. Surface settlement plates, pore pressure piezometers, and inclinometers were installed in the soft clay layer. The settlement and consolidation degree predictions employing one-dimensional consolidation, the Asaoka observational method, and pore water pressure data were analyzed. Back-calculation of flow parameters, comparison of soil properties before and after the first improvement were performed. The ground cracks and lateral movements induced by vacuum consolidation were also reported. After the first improvement, the properties of very soft clay were improved due to increased undrained shear strength and maximum pressure. In contrast, water content, void ratio, and compression index were reduced. The results illustrated that the vacuum-PVD improvement with an innovative field-distributed air–water separation system is effective for the second improvement of soft Bangkok clay.

Introduction

The soft marine Bangkok clay in Thailand covers an area of 80,000 km^2 with thicknesses of 10–20 m. The soft soil improvement technique by prefabricated vertical drains (PVD) is widely used because it is cheaper than the other techniques [1–9]. PVDs are artificially created vertical paths in the soft clay layer. This technique takes advantage of the higher horizontal permeability in the soft ground deposit. Excess pore water pressures created by preloading leads to preferential horizontal flow towards the PVDs and, along with it, vertically into the permeable layers generated by the hydraulic gradient. Thus, the PVD reduces the drainage path and shortens the time required to complete the consolidation process. However, installing the PVD with a mandrel creates a smear or disturbance in the soft clay surrounding the PVD circumference. This phenomenon causes a lower horizontal permeability in the smear zone [1, 2, 10, 11]. PVDs combined embankment preloading and vacuum pressure (called vacuum-PVD) have been used to accelerate the consolidation rate and reduce the instability of the soft clay. Kjellman [12] first proposed vacuum-PVD in the 1950s, and numerous

✉ Pitthaya Jamsawang
pitthaya.j@eng.kmutnb.ac.th

Dennes T. Bergado
bergado@ait.asia

Nuttapong Kovittayanon
ntp@ceteau.co.th

Francisco Baez
Francisco.baez@ceteau.com

Peter Tijl de Zwart
zwart@ceteau.com

1   Emeritus Professor and Project Consultant, Asian Institute of Technology, Bangkok, Thailand

2   Soil Engineering Research Center Director, Department of Civil Engineering, King Mongkut's University of Technology North Bangkok, Bangkok, Thailand

3   Ceteau (Thailand) Co. Ltd., Bangkok, Thailand

4   Ceteau BV, Makkum, The Netherlands

studies of vacuum-PVD have been subsequently continued up to the present [13–38], including clogging effects [14, 39–42].

Vacuum-PVD consolidation can minimize the pore pressure and keep constant total stress. The effective stress is increased by decreasing pore pressure (less than atmospheric) in the soft clay mass. Low shear strength and high compressibility of soft clay cause instability during construction and considerable consolidation settlement. These are the challenging tasks for geotechnical engineers in solving such problems. Preloading using PVD combined with surcharge and vacuum preloading is popular in the soft ground improvement method that has been applied in many countries. However, crucial inconsistency between field performances and design assumptions has existed, such as residual settlements after construction completion. Furthermore, there are still disagreements in horizontal consolidation coefficient (C_h) and smear effect. Even though soft Bangkok clay has been extensively studied for many decades, the back-calculated C_h values of soft Bangkok clay are significantly different. For example, the C_h value of 0.75 m^2/year was reported by Seah et al. [43], while the C_h values of greater than 3 m^2/year were derived by Balasubramaniam et al. [44] and Bergado et al. [45] for soft clay improved with PVD at the Second Bangkok International Airport (SBIA) site.

The vacuum pressure causes inward horizontal movements of the surrounding ground into the vacuum-PVD zone, resulting in ground cracks in the vacuum consolidation technique [20, 24, 46]. A certain vacuum pressure combined with embankment preloading can significantly reduce the lateral displacement of the soft clay and relieve the ground crack occurrences [15, 17, 24, 47]. Chai et al. [19] studied the behavior of PVD unit cells under vacuum pressure. After vacuum consolidation, horizontal compression and strain and higher effective stress, and higher shear strength developed near the PVD while horizontal extension occurred far from PVD. Surface settlements were not uniform. The periphery of the unit cell settled more than near the PVD. In the unit cell, non-uniform consolidation was found by Zhou and Chai [48].

Bergado et al. [45] indicated that microstructures of the vacuum-PVD improved soft clay were edge to face orientation and flocculated structure in the vertically dominated smear zone. Moreover, the microstructures of specimens in the horizontally dominated outside of smear zone exhibited mainly face to face orientation and dispersed microstructure and mixed face to face with edge to face orientations. The increasing intensities of edge to face microstructures were successfully correlated with increasing flow parameters and measured shear strengths within the smear zone.

This paper is concerned with the case study of the second improvement of the runway extension site at the Second Bangkok International Airport (SBIA). The vacuum-PVD technique with a combination of field-distributed air–water separation tanks and surcharge embankment preloading was applied. The SBIA is officially named Suvarnabhumi Airport. Thus, the subsoil of this project site is soft to medium stiff clay rather than very soft clay, which was caused by the first improvement. Focused on Zone 3, out of 16 Zones, consisting of an area of 27,544 m^2, this paper presents the predictions of settlements and degree of consolidations, and back-calculation of C_h values, and the observations of vertical and horizontal deformations and pore pressures.

Specifications and Discharge Capacity of PVD

Typical specifications of PVD are tabulated in Table 1. These specifications have been used for design by the Thailand Department of Highways, the Vietnam Ministry of Transportation, and the Federal Highway Administration. A discharge capacity is the essential function of PVDs. According to the ASTM standards, routine tests were performed using discharge capacity apparatus [49–53]. The PVD with a solid corrugated core is selected to prevent buckling and maintain the integrity of flow channels. In addition, the filter of the selected PVD is made of strong heat bonded geotextile, satisfying the filter and clogging criteria [54]. The filter surrounding the core allows the pore water entry but restricts the access of fine particles into the core

Table 1 General specifications of PVD

Properties	Test standard	Value			Unit
		DOH	FHWA	MOT	
Apparent opening size (O_{95})	ASTM D4751	≤90	≤75	≤75	μm
Grab tensile strength (whole PVD)	ASTM D4632	≥350	≥350	–	N
Tensile strength (whole PVD)	ASTM D4595	–	–	≥1000	N
Puncture resistance (filter only)	ASTM D4833	≥200	≥222	–	N
Discharge capacity at 7 days, 200 kPa and $i=1$	ASTM D4716	≥500	≥500	–	m^3/year

DOH Department of Highway—Thailand, *FHWA* Federal Highway Administration—USA, *MOT* Ministry of Transportation—Vietnam

body. At 20% of the corresponding straight condition, the lowest discharge capacity occurred when PVDs surrounded by soft clay particles simulated the actual field conditions under lateral pressures [55]. The lowest discharge capacity at 20% is 500 m^3/year when the discharge capacity at 2500 m^3/year is considered [53], which meets the minimum requirements as tabulated in Table 1.

Bergado et al. [56] investigated the proposed criteria of the PVD discharge capacity, including reduction factors as a result of creep, deformation and clogging (filtration). The summation of the reduction factors was approximately 10. Thus, the required discharge capacity is 50 m^3/year based on the minimum discharge capacity of 500 m^3/year, corresponding to the observed value [57]. Summarily, the PVD discharge capacity is not a primary factor because the minimum requirement is simply satisfied.

Flow Parameters and Smear Effect

The soft clay is generally in the NC state during the first PVD improvement. Therefore, the C_h value in NC state is used for estimating the consolidation rate. The C_h value can be determined from laboratory consolidation test, field cone penetration test with pore water pressure measurement, and back analysis of the existing data. However, it is challenging to determine the reliable C_h value in the NC state. The laboratory test results regularly provide underestimating the C_v and C_h values. In contrast, the C_h value derived from the field cone penetration tests is lightly in the OC state, which must be scaled down to the NC state. In design practice, the C_h value is frequently evaluated from the C_v value obtained from the laboratory tests by assuming the K_h/K_s value and utilizing the correlation of $C_h = (K_h/K_v)C_v$.

The back-analyzed C_h values from the observed settlement data based on the Asaoka method depend on the smear effects, including smear zone diameter, d_s, the ratio of $R_s = K_h/K_s$, and field discharge capacity of the drain, q_w. The well resistance can be negligible for the field q_w value of greater than 50 m^3/year. The d_s value is directly related to the equivalent mandrel diameter, d_m. The value of $d_s/d_m = 2$–3 is typically accepted [10, 58, 59]. However, the value of K_h/K_s is assumed from 1.4 to greater than 10 [10, 43, 60].

For soft Bangkok clay at the Second Bangkok International Airport site (SBIA), based on the measured settlement from three full-scale test embankments, with assumed values of $d_s/d_m = 2$ and $K_h/K_s = 5$, Balasubramaniam et al. [44] and Bergado et al. [3] obtained the minimum C_h value of about 3 m^2/year for the weakest soil layer from 4 to 8 m depth. Long et al. [28] reported a back-calculated C_h value of 4 m^2/year using similar smear effects combined with the Asaoka method. The flow parameters coupled with the consolidation settlement of 1.50 m correspond to the results from the first

PVD improvement. The design of the second improvement used $C_h = 4$ m^2/year.

Settlement Calculations

Primary Settlement

Based on a one-dimensional (1-D) consolidation test, the final primary settlement, S_{oed}, can be derived as follows:

$$S_{oed} = \sum h \left[RR \log \left(\frac{\sigma'_p}{\sigma'_{vo}} \right) + CR \log \left(\frac{\sigma'_{vf}}{\sigma'_p} \right) \right], \qquad (1)$$

where h is the subsoil thickness, CR is the compression ratio, RR is the re-compression ratio, σ'_{vo} is the existing overburden pressure, σ'_p is the pre-consolidation pressure, and σ'_{vf} is the final vertical effective stress.

The total primary settlement of the soft clay layer comprises the primary consolidation settlement induced by an increase in the effective stress, S_{cf}, and immediate settlement induced by undrained deformation, S_i. Thus, the following expressions have been used for soft clays:

$$S_{cf} = \mu_c S_{oed}, \; S_i = (1 - \mu_c) S_{oed}, \qquad (2)$$

where S_{oed} is the 1-D consolidation settlement, μ_c value is between 0.8 and 1.0, depending on various factors such as soft clay thickness, embankment width, OCR, and preloading method.

The primary consolidation settlement of soft clay subjected to the embankment loading can be computed applying Eqs. (1) and (2) and the σ'_{vf} value can be calculated as follows:

$$\sigma'_{vf} = \sigma'_{vo} + \Delta\sigma_v + (u_o - u_f), \qquad (3)$$

where $\Delta\sigma_v$ is an increase in the total vertical induced by the embankment load and permanent loads applying on the ground surface, u_0 is the initial pore water pressure before constructing embankment), u_f is the final excess pore water pressure. The u_f can be smaller than the u_0 for the case of pore pressure drawdown caused by the groundwater pumping.

Consolidation with PVD

The degree of consolidation, U, can be estimated using Eq. (4) proposed by Carrillo [61], as follows:

$$U = 1 - (1 - U_h)(1 - U_v), \qquad (4)$$

where U_h and U_v are the degree of consolidation in horizontal and vertical directions, respectively. U_v can be neglected

for the PVD improved zone because most of the consolidation drainage occurred horizontally. The U_h is zero for the underlying unimproved soil layers (without PVD).

The solution for calculating the U_h of PVD improved soft ground was given by Hansbo [1] as follows:

$$U_h = 1 - e^{\left(\frac{-8T_h}{F}\right)} \tag{5}$$

$$T_h = \frac{C_h t}{D_e^2} \tag{6}$$

$$F = F_n + F_s + F_r \tag{7}$$

$$F_n = \frac{n^2}{n-1}\ln n - \frac{3n^2-1}{4n^2} \cong \ln\left(\frac{D_e}{d_w}\right) - \frac{3}{4} \tag{8}$$

$$F_s = \left(\frac{K_h}{K_s} - 1\right)\ln\left(\frac{d_s}{d_w}\right) \tag{9}$$

$$F_r = \pi z(2L - z)\frac{K_h}{q_w} \tag{10}$$

$$d_w = \frac{1}{2}(a + b), \tag{11}$$

where D_e is the equivalent diameter of a unit PVD influence zone, K_s is the horizontal permeability of soft clay in the smear zone, z is the distance from the drainage end of the drain, L is the length PVD for one-way drainage and is half of PVD length for drainage boundary at both ends of PVD, q_w is the in-situ discharge capacity of the PVD, d_w is the equivalent diameter of PVD, a and b refer to PVD thickness and PVD width, respectively, d_s is the equivalent diameter of the smear zone induced by installing PVD and d_m is the equivalent diameter of the mandrel. The correlation of d_s and d_m was proposed by Hansbo [58] as follows:

$$d_s = 2d_m \tag{12}$$

$$d_m = 2\sqrt{\left(\frac{wl}{\pi}\right)}, \tag{13}$$

where w and l correspond to the mandrel width and mandrel thickness, respectively.

In practical cases, the K_h/q_w value in Eq. (10) is frequently lower than 0.0001. Thus, the value of F_r is negligible compared with F_n and F_s values, and the F_r has an insiginificant effect for the field q_w value of greater than 50 m³/year [3, 44, 57, 61]. Thus, the main factors affecting the calculated consolidation rate consist of the C_h, $R_s = K_h/K_s$, and d_s/d_m, which have to be confirmed for the specific project site.

Consolidation Settlement at Time *t* during Preloading

The consolidation settlement at time t during the preloading stage, S_{ct}, can be calculated based on the corresponding consolidation degree, U_t, and the final consolidation settlement, S_{cf}, under preloading load.

$$S_{ct} = U_t S_{cf} \tag{14}$$

The value of S_{cf} is derived using Eqs. (1) and (2).

The σ'_{vf} value for PVD improvement without vacuum pressure is calculated as follows:

$$\sigma'_{vf} = \sigma'_{vo} + \Delta\sigma_v, \tag{15}$$

where $\Delta\sigma_v$ refers to the increased vertical stress induced by the embankment stress, p_{fill}, applied on the ground surface.

$$p_{fill} = \sum \gamma_{fill} h_{fill} - \gamma_w h_w, \tag{16}$$

where γ_{fill} refers to the total unit weight of the fill materials, h_{fill} is the fill layer thickness, γ_w is the water unit weight, and h_w is the fill layer thickness located below the groundwater table during the preloading time.

For vacuum PVD using direct tubing system (without airtight membrane):

$$\sigma'_{vf} = \sigma'_{vo} + \Delta\sigma_v + p_{vac}, \tag{17}$$

where p_{vac} is the effective vacuum pressure.

The σ'_{vf} can be evaluated by Eq. (17) for the vacuum PVD with an airtight membrane. However, the $\Delta\sigma_v$ should be obtained from $p_{fill} = \sum \gamma_{fill} h_{fill}$ because the pore pressure in the embankment fill under the airtight membrane is negative.

Secondary Compression

The secondary compression is the small magnitude for the improved clay layer after the completion of primary consolidation. From the 1-D consolidation test, the secondary compression settlement, S_s, at time t can be calculated as follows:

$$S_s = hC'_{\alpha\varepsilon}\log\left(\frac{t}{t_p}\right), \tag{18}$$

where $C'_{\alpha\varepsilon}$ is the secondary compression ratio, and t_p is the time at the end of primary consolidation. The secondary compression can be ignored for the soft clay without improvement due to its small magnitude. Moreover, the time to complete the primary consolidation settlement is greater than the project's lifetime. The time to reach 90% of consolidation is approximately one year for the soft ground

improved with PVD. Therefore, $t_p = 1$ year is frequently used for estimating the residual compression of soft ground enhanced with PVD. The $C_{\alpha\varepsilon}$ value can be taken at NC to OC state, depending on the loading conditions of the underlying soft clay during the operation period.

Settlement Control

Asaoka's method [63] is commonly used for estimating the settlement versus time using the actual observed settlement data. The 1-D consolidation equation is expressed in a first-order estimation as follows:

$$S_t = S_f\left(1 - e^{\lambda t}\right), \tag{19}$$

where S_t refers to consolidation settlement at time t, S_f is the primary consolidation settlement, and λ is a constant value. Equation 19 was derived by Asaoka [63], expressed as a solution of the following differential equation:

$$\frac{dS}{dt} - \lambda S = f, \tag{20}$$

where f is an unknown constant.

Based on Eq. (20), the time is equally divided into the interval of Δt. The following equations are obtained:

$$S_n = \beta_0 + \beta_1 S_{n-1} \tag{21}$$

$$\beta_1 = \frac{1}{1 - \lambda \Delta t} \tag{22}$$

$$\beta_0 = f\beta_1, \tag{23}$$

where S_k and S_{k-1} are the settlements at time $t = t_k$ and time $t = t_k - \Delta t$, respectively.

β_0 and β_1 from Eq. 21 can be derived from the intercept and the slope of the best fitted straight line of $(S_k \sim S_{k-1})$ plot, respectively. As time approaches infinity, $S_k = S_{k-1} = S_f$; then

$$S_f = \frac{\beta_0}{1 - \beta_1} \tag{24}$$

Based on Eqs. (5), (19), and (22), the following equation can be obtained to derive the C_h value, which is often used for its back analysis based on monitored settlement data. From Eqs. (5), (19), and (22), the following equation can be derived to obtain the coefficient of horizontal consolidation (C_h), which is frequently employed for the back analysis based on the observed settlement data.

$$C_h = \frac{(1 - \beta_1)d_e^2 F}{8\beta_1 \Delta t} \tag{25}$$

As indicated in Eq. 25, the C_h value depends on the time interval Δt. Asaoka [63] recommended a larger time interval for more accurate results, and thus, the time interval Δt of 21 days was used.

Project Description

Site Conditions and Soil Properties Before and After First PVD Improvement

The site is located approximately 30 km southeast of Bangkok at the SBIA land in the Central Plain of Thailand with an area of 8 by 4 km (Fig. 1). As part of the SBIA expansion

Fig. 1 Location of runway extension test site
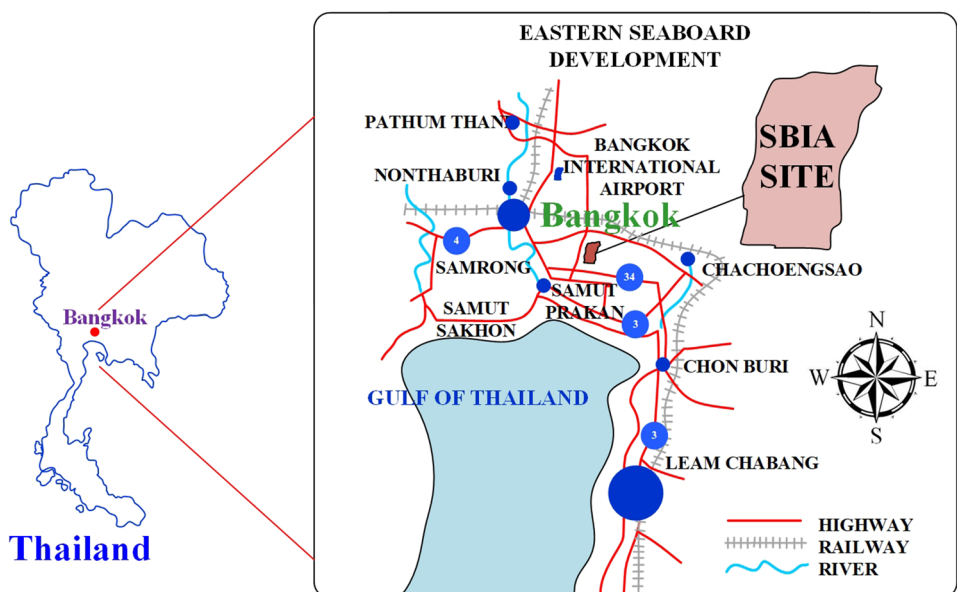
plan, the runway extension and the locations of boreholes and field vane tests are shown in Figs. 2a and b, respectively. The project site is subdivided into 16 different zones, which have been partially improved by PVD in the previous project. This paper is focused on Zone 3 (see Figs. 2a and b) since this zone was performed first. As shown in Fig. 3, the soil profile consists of approximately 2–4 m thick sand and rockfill overlying soft to medium clay of approximately 12 m thickness followed by a stiff clay layer around 8–10 m thickness, which is in turn underlain dense to very dense sand. The dummy pore pressures were obtained at the unloaded part of the site located away from the improvement area. The dummy piezometer readings (Fig. 4) represent the

initial pore pressures conditions before Preloading. Figure 4 demonstrates the pore pressure drawdown due to excessive withdrawal of groundwater from underlying aquifers that caused ground subsidence. Thus, the PVDs should be limited in length to be installed only above the pore pressure drawdown area.

The index and engineering properties of the underlying clay before and after the first improvement are shown in Tables 1 and 2, respectively. Before the first improvement, the underlying soil layers consisted of very soft to soft clay with average liquid limit values and water content of more than 100%t. After the first improvement, the average liquid limit values and water content were reduced to
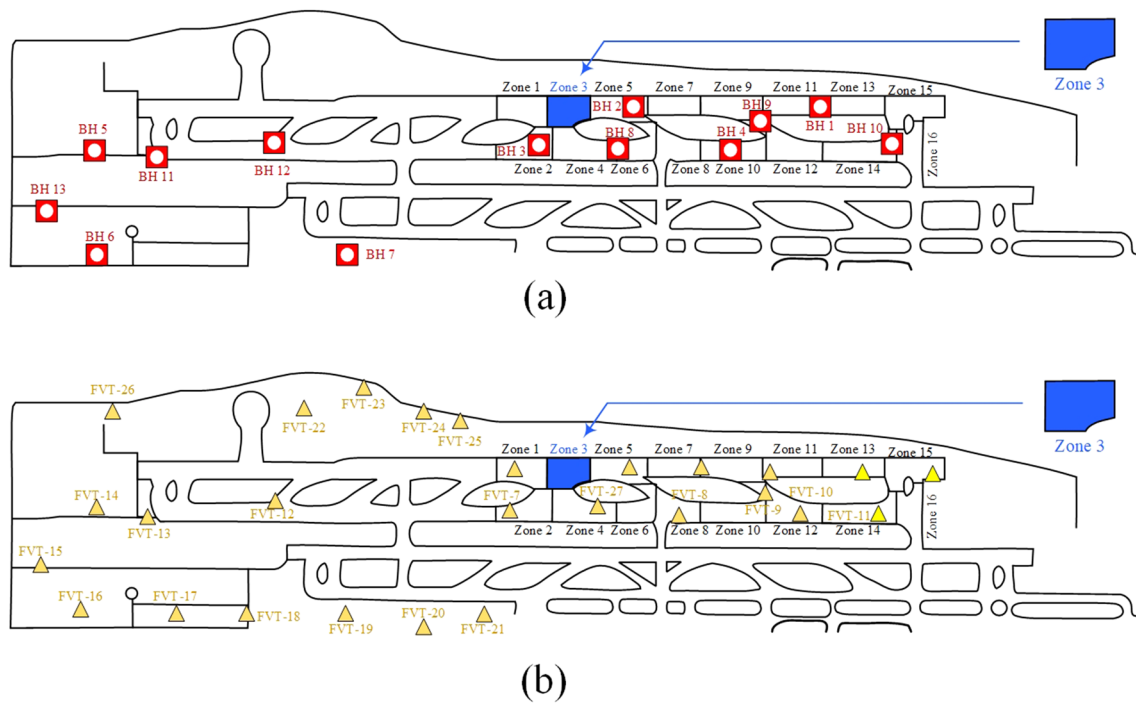

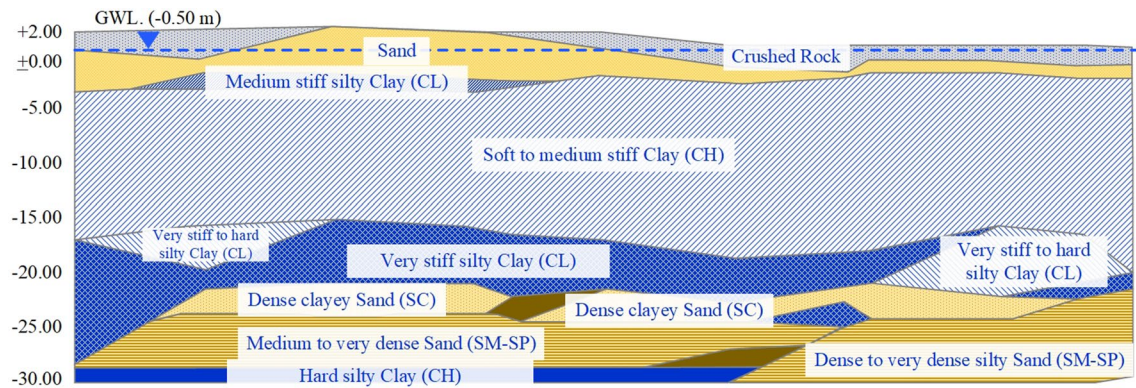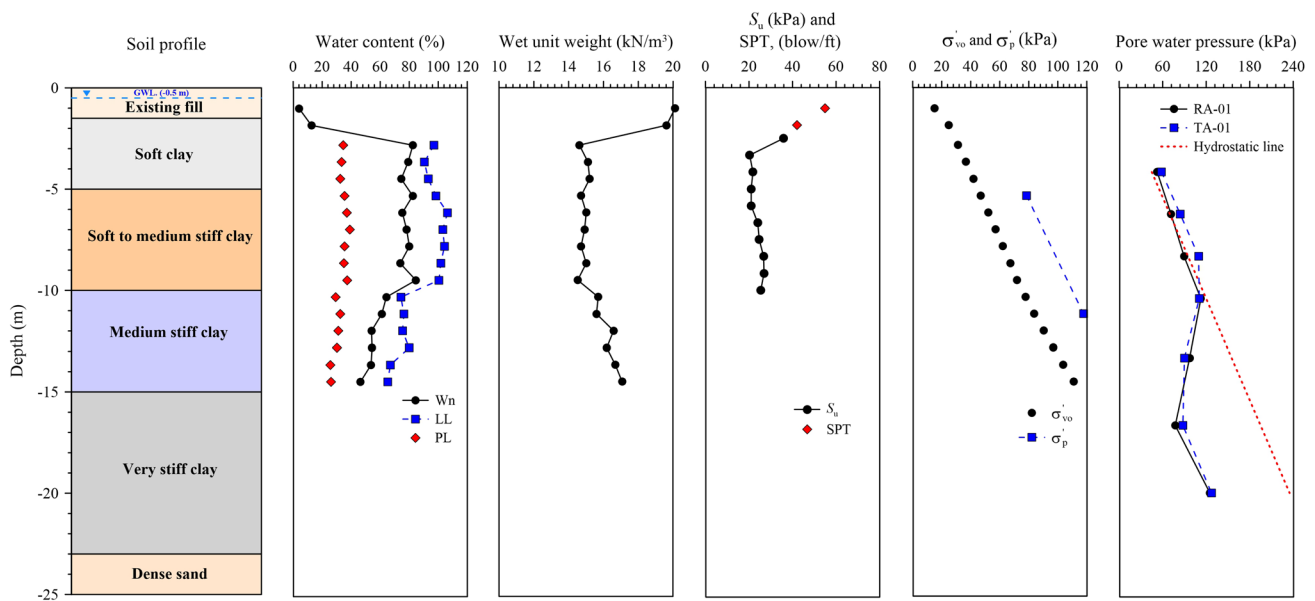Fig. 2 Locations of **a** boreholes and **b** field vane shear tests at the runway extension site

Fig. 3 Variation in the soil profiles of at the runway extension site

Fig. 4 Soil properties after the first improvement

Table 2 Index properties of underlying clay layers (Before and after 1st improvement)

| Depth (m)	− 2 to − 10	− 4 to − 10
Soil properties	Very soft to soft clay (Before 1st improvement)	Soft to medium-stiff clay (After 1st improvement)
Unit weight (kN/m³)	14	15
Water content (%)	90–110	70–80
Liquid limit (LL)	90–120	89–106
Plastic limit (PL)	40–45	33–39
Soil classification (USCS)	CH	CH

100 and 80%, respectively. Moreover, the undrained shear strengths obtained from corrected field vane tests increased from 8–12 kPa to 20–27 kPa, and the maximum past pressures rose from 40–60 kPa to 78–118 kPa. As expected, the compression and recompression ratios did not change much, but the void ratios decreased while the overconsolidation ratios (OCR) increased. The water contents, liquid limits, plastic limits, unit weights, undrained shear strengths, and maximum past pressures after the first PVD improvement are also plotted in Fig. 4.

## Second Vacuum-PVD Improvement Procedures and Monitoring Instrumentations

After the first improvement with PVD, the underlying clay layers were pre-compressed by as much as 1.50 m. Then, the surcharge embankment was excavated and moved to an

adjacent site. The site conditions and soil properties were mentioned earlier in the previous section. It can be seen that the average undrained shear strength increased up to 27 kPa and the average maximum past pressure increased from 40 to 80 kPa together with the reductions of water contents and void ratios. As part of the runway extension project, there is a need to increase the maximum past pressure to more than 100 kPa. Subsequently, the second improvement works were implemented consisting of vacuum PVD with airtight membranes (VCM-MH). The PVD elements were connected to the horizontal drains in the sand blanket at the ground surface to accelerate the consolidation. The configuration of PVD installations is indicated in Fig. 5.

The 10 m-long PVDs with 1.0 m spacing in the square pattern were installed from the 0.5 m-thick sand drainage blanket (equivalent to 10 kPa surcharge), through 1.5 m existing fill, to − 10 m elevation. The third layer of
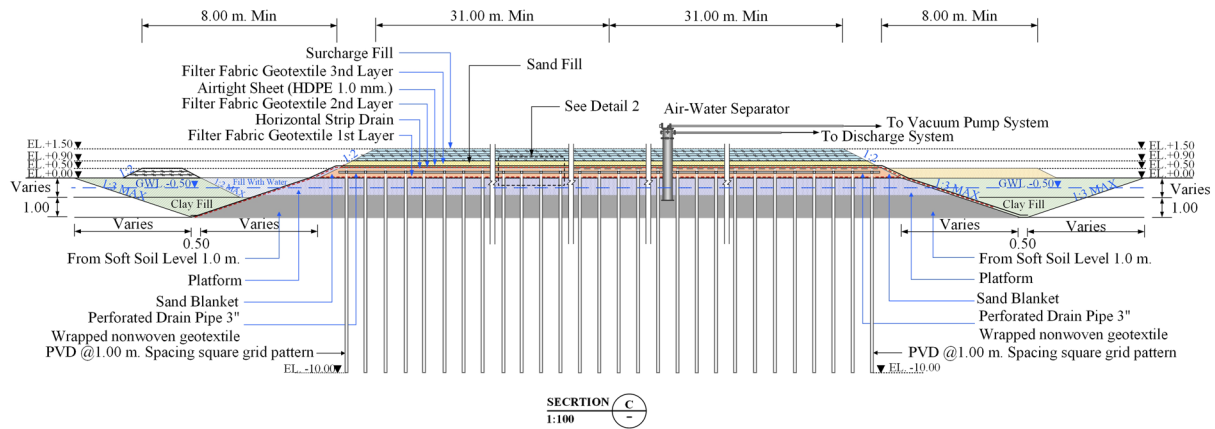
(a) PVD installation
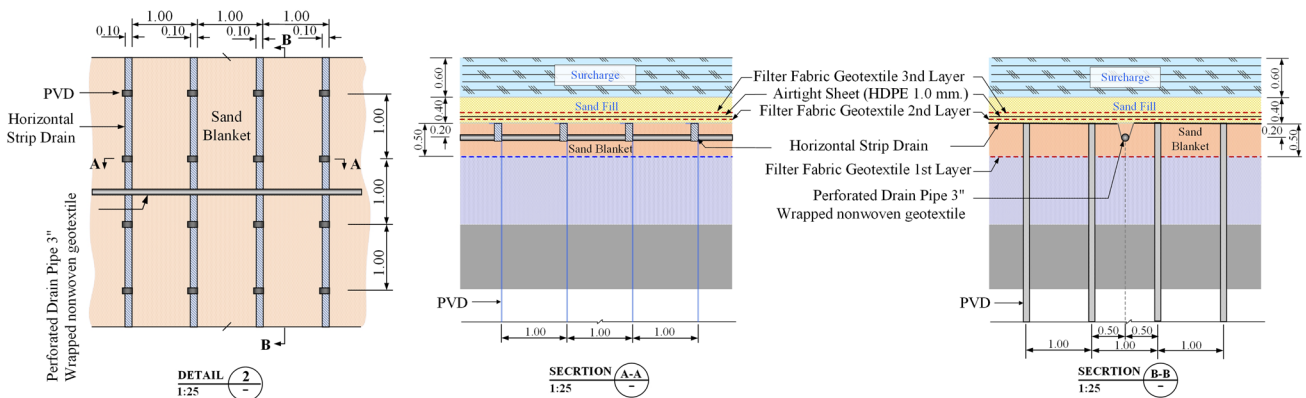
(b) PVD connections with horizontal drain and perforated pipes

Fig. 5 Details of PVD installation

nonwoven geotextiles in Fig. 5 was used for separation and protection. As previously mentioned, the horizontal drainage at the sand blanket was provided by horizontal band drains. An additional 1.0 m-thick surcharge fill equivalent to 20 kPa was added on top of the sand blanket. Moreover, at the end of vacuum PVD loading, an additional 30 kPa fill with the pavement will be added. The PVD installation commenced on 3 January 2021, and the vacuum preloading was started on 29 April 2021 with a full surcharge a month later.

The PVD utilized in this case study has a cross-section of 100×4 mm and has a filter permeability of greater than 1×10^{-4} m/s. The general PVD properties are presented in Table 3. The typical cross-section of the new vacuum-PVD system is shown in Fig. 6a, together with the relevant photographs. The connection between PVDs and the horizontal strip drains is within the 0.5 m-thick sand blanket (Fig. 6b). The vacuum pressures were consistently generated by vacuum pumps and efficiently assisted by the field-distributed air–water separation tank (Fig. 6c). The geomembrane layer

Table 3 Engineering properties of underlying clay layers (Before and after 1st improvement)

Parameters	Before 1st improvement	After 1st improvement
Compression ratio (*CR*)	0.20–0.40	0.26–0.35
Recompression ratio (*RR*)	0.02–0.04	0.028–0.034
Initial void ratio (e_o)	3–4	2.2–2.5
Overconsolidation ratio (*OCR*)	1.0–1.5	1.4–1.8
Corrected vane shear strength (S_{uv}), kPa	8–12	20–27
Maximum past pressure, $\Delta\bar{\sigma}_{vm}$ (kPa)	40–60	78–118
Permeability coefficient, k (m/s)	–	2.43×10^{-10}

(a) Typical cross section of the improved air-water separation system

(b) Connection of PVD with horizontal drain

(c) Air-water separation tank with vacuum meter

(d) Placement of geotextiles and geomembranes

(e) Perforated pipe connection
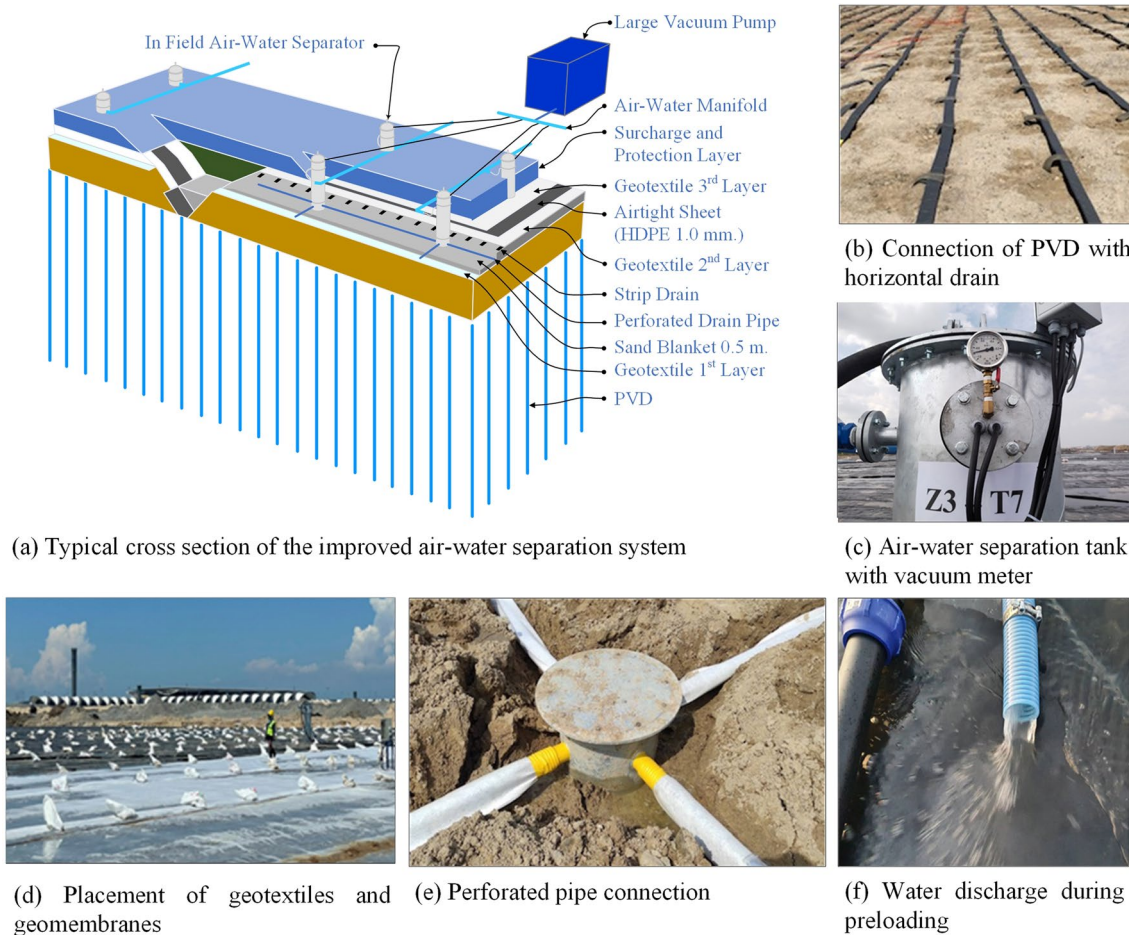
(f) Water discharge during preloading

Fig. 6 The modified air–water separation system used in this project

(sealing layer) was placed on top of the sand blanket layer. Three layers of geotextiles were also installed below and above the geomembrane as protection against puncture (Fig. 6d). The horizontal strip drains were connected to the perforated pipes and the vacuum pump (Fig. 6e), and pore water discharges can be observed (Fig. 6f).

Figure 7 illustrates the layout of the monitoring instruments consisting of surface settlement plates, pushed-in and bored piezometers, and inclinometers. The surface settlement plate was made of a 16 mm-diameter riser steel rod welded to a square-base steel plate with a size of 0.4×0.4 m and thickness of 3 mm. Optical leveling measurements to the top of the riser provide a record of plate elevations. A collimation error should be smaller than the allowable one of 1/20,000. Two types of GEOCON piezometers were utilized to monitor pore water pressure induced by the vacuum pressures, including pushed-in and bored piezometers. Both types have similar specifications, such as a standard range of -100 kPa, resolution of 0.025% full-scale range, and an accuracy ± 0.1% full-scale range. The model 4500DP pushed-in piezometer has

the transducer located inside a housing with a drill rod thread and removable pointed nose cone. This model is ideally suited for use in peat and soft clays. The model 4500 bored standard piezometer is designed to measure fluid pressures such as groundwater elevations and pore pressures when installed inside boreholes and observation wells. The pushed-in and bored piezometers monitored the pore water pressure at -5 m and -10 m elevations.

The GEOCON digital inclinometer system was used to motor the lateral displacement profiles of the improved ground during the vacuum preloading. The system includes a model 6100D digital inclinometer probe, a reel-mounted cable, and a readout data logger. The inclinometer casing used in this project was a 65 mm-diameter plastic pipe. The probe has a standard range of $\pm 30°$, resolution of $0.0013°$, and accuracy of ± 3 mm/30 m. The inclinometer casings were installed up to the stiff clay layer at a depth of 19 m, which is sufficient to obtain a zero reading at this depth based on the practical work. The piezometers and settlement plates were installed at locations RA-01, TA01,

Fig. 7 Location of monitoring instrumentations for Zone 3 of runway extension site
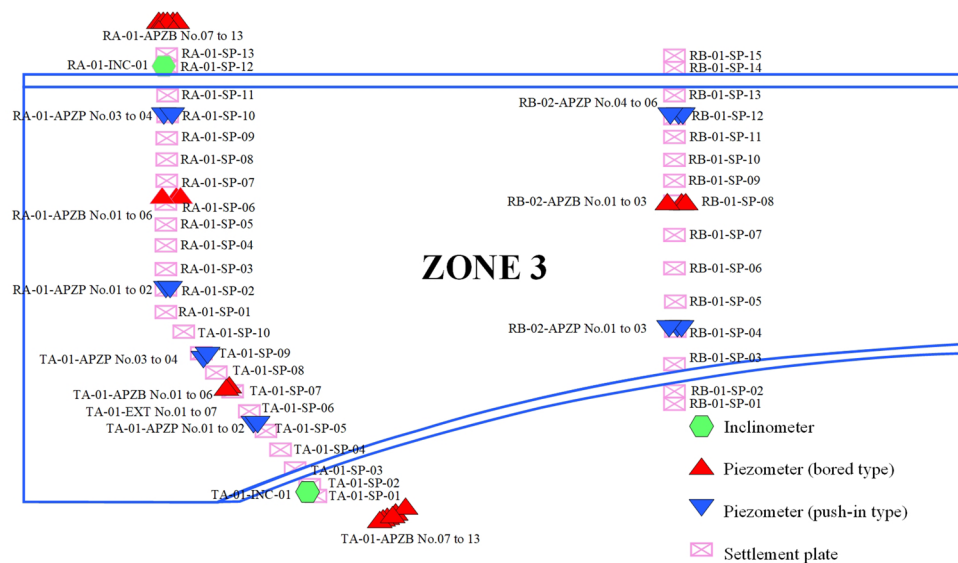
and RB-02. Two inclinometers were installed at locations RA-01 and TA-01.

Loading Stage by Surcharge Load and Vacuum Pressure

In Zone 3, the 30-kPa surcharge load and 80 to 90 kPa vacuum pressure with time are presented in Fig. 8a. The 30-kPa surcharge load induced by the 0.5 m-thick sand blanket and 1.0 m-thick fill layer were added to the 90-kPa vacuum pressure. The field-distributed air–water separators were very efficient in consistently generating the vacuum pressures underneath the sealing geomembranes. However, variations in vacuum pressures at the initial stage during the saturation process of embankment fill above the water table were observed, and problems related to preliminary salt clogging for the pump filter were also detected. After the blockage problem was successfully solved, the vacuum pump consistently and efficiently maintained the vacuum pressure aided by the field-distributed air–water separation devices, as mentioned previously.

Data Analyses

Measured Surface Settlements

The surface settlement versus time and settlement rate versus time curves are presented in Fig. 8b and c, respectively. The surface settlements and settlement rates increased rapidly and subsequently decreased with time during the preloading period. The surface settlements and settlement rates were currently measured at around 600 mm and 4 mm/day, respectively.

Negligible amounts of rebound can be further observed later up to one month after stopping the vacuum pressures.

Observed Porewater Pressures with Time

As plotted in Fig. 8a, the loading at the sand blanket below the airtight membranes consisted of 80–90 kPa vacuum pressures and 30 kPa surcharge pressure. The generated porewater pressures in the underlying clay layer at − 5 m and − 10 m elevations, as presented in Fig. 8d and e, respectively, consisted of − 50 to − 60 kPa and − 40 to − 50 kPa. These piezometers were installed in between the PVD locations with a spacing of 1.0 m in a square pattern. The measured pore pressures at − 10 m elevation were slightly lower than the corresponding observed values at − 5 m elevation. The pore pressures were expected to reduce with depth slightly.

In Zone 3, the generation of pore pressures with time at different depths is illustrated in Fig. 9, which were measured from bored type piezometers at locations RA-01, RB-02, and TA-01. Because of the loading vacuum pressures of 80–90 kPa and embankment surcharge of 30 kPa, pore pressure values of − 50 to − 60 kPa were created at − 5 m elevation and slightly decreased from − 40 to − 50 kPa at − 10 m elevation. These piezometer readings were similar to the previous illustrations with time in Fig. 8d and e. Logically, the pore water pressures reduced slightly with depth.

Lateral Displacements and Ground Cracks

The lateral movement profiles of subsoils in Fig. 10 for locations RA-01 and TA-01 moved inward perpendicular to the embankments. The maximum lateral movement of 180 mm

Fig. 8 a Vacuum pressure and surcharge, **b** surface settlement, **c** excess pore water pressurat -5.0 m depth, **d** excess pore water pressure at − 7.5 m depth, and **e** excess pore water pressure at − 10.0 m depth (Note: solid line = pushed in type; dashed line = bored type)
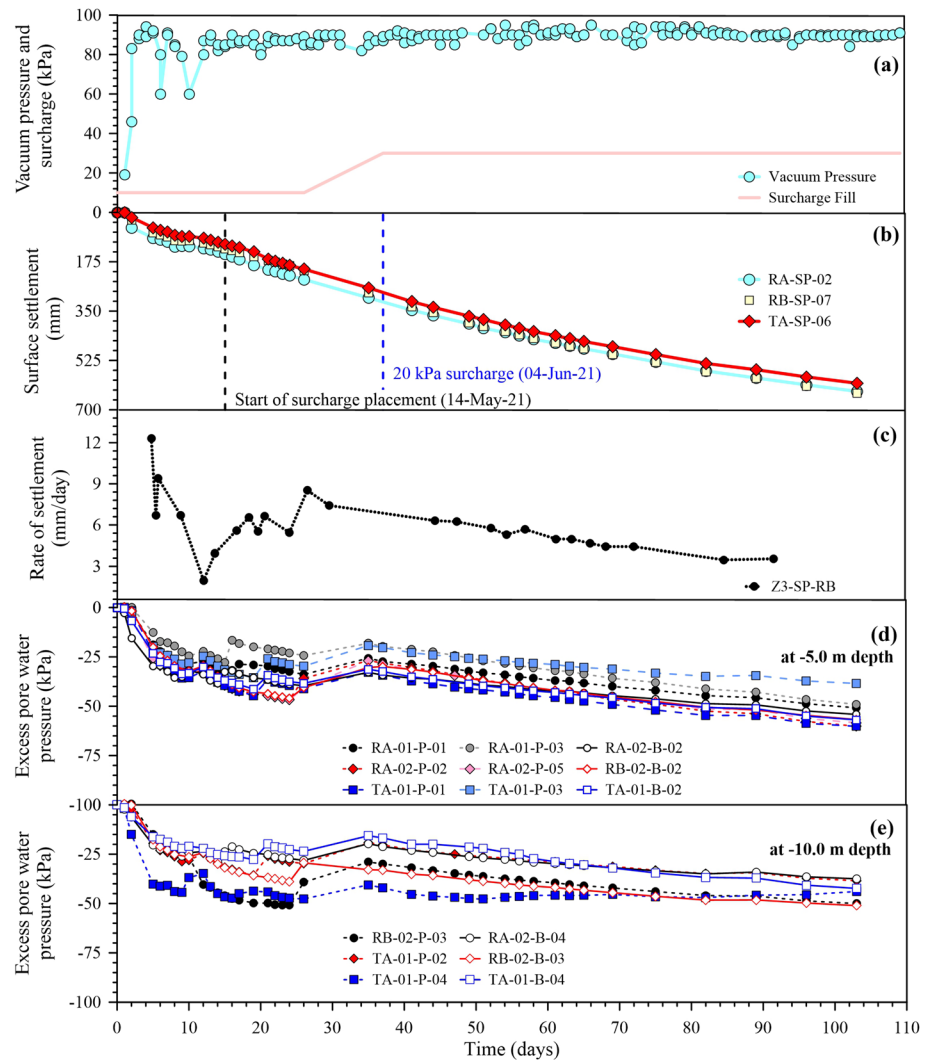
was observed at the current preloading stage because of the higher vacuum pressures than the embankment surcharge stresses [47]. Chu et al. [20] reported the maximum lateral displacement of 500 mm for the vacuum-PVD improvement project with similar magnitudes of vacuum and surcharge pressures. Similar investigations were also conducted in many projects [5, 8, 25, 40, 65].

Ground cracks were detected at a distance of about 6 m from the trench edge of the sealing membrane area, as shown in Fig. 11. The ground cracks specified larger vacuum pressure than the horizontal soil pressures, causing inward lateral displacement. The ground crack depth (z_c) can be derived utilizing the active soil pressure, soil strength parameter and groundwater level, according to Chai et al. [47], as follows:

$$z_c = \frac{2c'}{\gamma_t \sqrt{k_a}}, \text{ for } z_c < z_w$$

$$z_c = \frac{1}{(\gamma_t - \gamma_w)}\left[\frac{2c'}{\sqrt{k_a}} - \gamma_w z_w\right], \text{ for } z_c > z_w$$

(26)

where z_w = groundwater level below the ground surface, γ_t = total unit weight of soil, γ_w = unit weight of pore water, c' and ϕ' = effective cohesion and friction angle of soil, respectively, and k_a = active earth pressure coefficient = $\tan^2(45-\phi'/2)$. Assuming $c' = 5$ kPa and $\phi' = 23°$, $\gamma_t = 15.8$ kN/m³, and $z_w = 0.5$ m, Eq. (26) predicts $z_c = 4.36$ m from the existing ground surface. The crack depths could correspond to the observed lateral displacement profiles, as
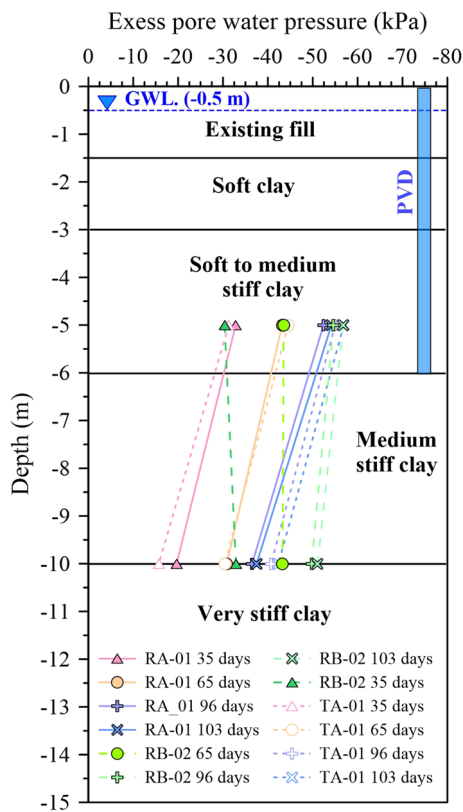
Fig. 9 Excess pore water pressures with time and depth in Zone 3 measured from bored type piezometers

$$U = 1 - \frac{\int_0^{h_{dr}} \left[u_t(z) - u_s(z) \right] dz}{\int_0^{h_{dr}} \left[u_0(z) - u_s(z) \right] dz} \tag{27}$$
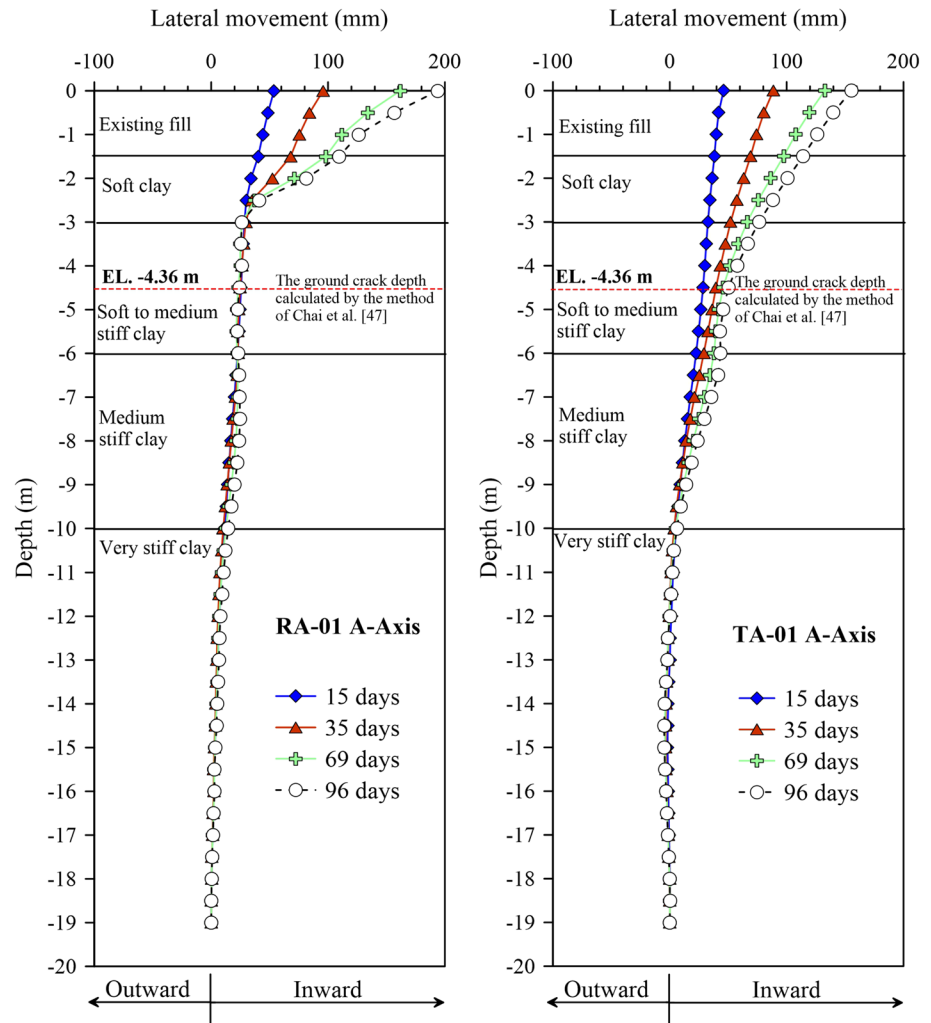
$$u_s(z) = \gamma_w z - u_s,$$

where $u_0(z) =$ initial pore water pressure at depth z, $u_t(z) =$ pore water pressure at depth z and time t, $u_s(z) =$ vacuum pressure at depth z, $u_s =$ vacuum pressure applied (typically 80 kPa); $h_{dr} =$ drainage path. If $u_s = 0$, the above equations can be used for fill preloading. Since the vacuum-PVD Preloading is still going on, the DOC predictions from the Asaoka method and 1-D consolidation are compared in Table 6 using the current values of observed settlements. The DOC estimated by the Asaoka method also agreed with the corresponding values calculated by the 1-D consolidation method and the excess pore water pressure data.

Following the Asaoka method [63], the C_h values were back-analyzed and plotted in Fig. 13 for Zone 3 [63]. In Fig. 13, along the line of $d_s/d_m = 2$, the DOC are predicted using Hansbo method as tabulated in Table 7 corresponding to three pairs of flow parameters, namely the following: $K_h/K_s = 3$ with $C_h = 4.1$, $K_h/K_s = 4$ with $C_h = 5.1$, and $K_h/K_s = 5$ with $C_h = 6.2$. Interestingly, the plots of DOC with time coincide in one line, as illustrated in Fig. 14. It can be seen that the predicted time to 90% DOC at a spacing of 1.0 m in the square pattern is about 5.3 months (0.44 years) which satisfied the design requirements of approximately 90 percent DOC (U ≥ 90%) in 5.3 months (0.44 years).

During the first ground improvement using conventional PVD with $d_s/d_m = 2$ and $K_h/K_s = 5$, the average back-calculated C_h values of 2 to 4 m²/year were derived. Bergado et al. [8, 57] also reported a similar C_h value of 3 m²/year obtained from the adjacent SBIA project utilizing a traditional PVD improvement method. However, the K_s value for vacuum-PVD technic can slightly increase. Thus, the ratio, K_h/K_s, can also slightly decrease. Based on the back-calculations of settlement rates obtained from soft clay improved with vacuum-PVD, Artidteang et al. [66], Lam et al. [26], Long et al. [30], Saowapakpiboon et al. [32–34], and Bergado et al. [67] obtained a slight reduction of K_h/K_s because of the increased K_s within the smear zone and a slight increase in K_h (outside the smear zone). Bergado et al. [45] derived flocculated microstructures with a high degree of edge to face orientation within the smear zone and a low degree outside the smear zone. The flocculated microstructure is related to the increased K_s with consequent slight reduction of K_h/K_s and the associated increase in C_h values. Thus, using the Asaoka method with $K_h/K_s = 3$ and $d_s/d_m = 2$, the back-calculated value of $C_h = 4$ m²/year is obtained in Fig. 13 and plotted in Fig. 14 for the second improvement using Vacuum-PVD in the runway extension project.

shown in Fig. 10. The maximum lateral displacement could amount to 10% of the settlement observed by other investigators [5, 8, 25, 35, 64].

Prediction of Ultimate Settlements, Consolidation Degree, and Back-Calculation of C_h Values

For Zone 3, the Asaoka plots [58] are shown in Fig. 12 to derive the ultimate settlement. The predicted ultimate settlement of 0.81 m based on the Asaoka method [63] generally agreed with the corresponding 1-D consolidation settlement prediction of 0.79 m with 100 kPa vacuum pressure and surcharge load as tabulated in Table 4. With increased vacuum and surcharge load to 110 kPa and the designer's parameters, the 1-D consolidation settlement prediction of 0.81 m is tabulated in Table 5.

The degree of consolidation (DOC) of soil under vacuum preloading can also be calculated, based on the excess pore water pressure data, as follows [65]:

Fig. 10 Lateral movement profiles in Zone 3

Secondary Settlements

For OC clays, the secondary compression ratio, $C'_\alpha = 0.04$ $(C_r/(1+e_0)) = 0.04$ (RR) where RR is the recompression ratio. If $RR = 0.05$, then $C'_\alpha = 0.002$. Since $t_s = 10 \, t_p$, then $\log t_s/t_p = 1$. The simplified soil profile and PVD zone of the Vacuum-PVD runway extension project are shown in Fig. 15. The groundwater table is located at a -0.5 m elevation. The PVDs were installed through a 1.5 m-thick old fill from the first improvement project to -10 m elevation within the soft to medium clay layer. Below the PVD installation lies the unimproved 5 m-thick medium stiff clay layer followed by a stiff clay layer. In Fig. 15, the thickness of the clay layer, $h = 13.5$ m, then the S_s in 10 years is given as: $S_s = C'_\alpha(h) = 0.002$ (13.5 m) (1000) = 27 mm or 0.027 m.

Prediction of Settlements with Time

Using the current average settlements at locations RA-01, RB-02, and TA-01, the settlement with time can be predicted using the Asaoka and 1-D consolidation methods as plotted in Fig. 16. The corresponding degrees of consolidation (DOC) are tabulated in Table 6 with an average value of 74%. Using the predicted degree of consolidation (DOC) by Hansbo method as indicated in Table 7 and the 1-D consolidation settlement assuming 100 kPa surcharge load as tabulated in Table 4, the predicted settlement with time can be plotted as shown in Fig. 17. The 100 kPa surcharge load is the sum of 70 kPa vacuum pressure and embankment surcharge of 30 kPa. The flow parameters used in Table 7 consist of $K_h/K_s = 3$ and $C_h = 4.05$ m²/year. After

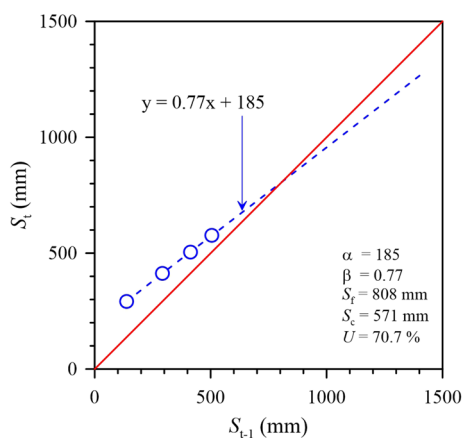**Fig. 11** Photographs of the ground cracks in Zone 3

Fig. 12 Asaoka plot for TA-01 with time interval $\Delta t = 21$ days to obtain the ultimate settlement

the second vacuum-PVD improvement, when the vacuum pressure stopped and only 60 kPa surcharge load remained, the 1-D consolidation settlement of the improved clay layer up to 15 m thickness was obtained as 0.265 m, as shown in Table 8. The predicted compression from − 1.5 to − 10 m depths as tabulated in Table 8 amounted to 0.06 m which

constitutes the compression after the second vacuum-PVD improvement.

Moreover, as shown in Table 8, the predicted compression in the underlying and unimproved medium stiff clay layer from 10 to 15 m depth (Fig. 17) amounted to 0.20 m. Using $C_v = 2$ m^2/year, and assuming 1-D vertical drainage, the predicted settlement with time, after the vacuum was stopped, is also plotted in Fig. 17, where the end of consolidation was indicated after 10 years. If the secondary compression of 0.027 m together with the compression of 0.06 m from − 1.5 to − 10 m elevations in the improved overconsolidated layer is added together (see bottom of Fig. 17), the total compression at 10 years after the second vacuum-PVD improvement amounted to 0.29 m < 0.30 m which is within the design specifications. Furthermore, the 1-D consolidation settlement with 110 kPa loading (80 kPa vacuum pressure and 30 kPa surcharge) amounted to 0.81 m as tabulated in Table 5, which corresponds to the predicted settlement with time plot by the design as shown in Fig. 18 within the design specifications.

Conclusions

The previous first improvement using PVD combined with embankment surcharge pre-compressed the underlying compressible clay layer by 1.5 m and transformed from very soft to soft clay into soft to medium stiff clay layer with maximum past pressure of 80–83 kPa. There is a need to increase the maximum past pressure to more than 100 kPa for the runway extension project. Thus, the second vacuum-PVD improvement was implemented to accelerate the consolidation. The second soft ground improvement performance, including settlement predictions, flow parameter calculations, and comparisons of soil properties after and before improvement, has been reported. Based on the field and analysis results, the main conclusions can be drawn, as follows:

1. This presentation is focused on Zone 3 of the test site with an area of 27,544 m^2 which is part of the runway extension project. The runway extension project was divided into 16 Zones. The groundwater table was located at a − 0.5 m elevation below the original ground surface. The 10 m-long PVDs were installed to a depth of − 10 m with a spacing of 1.0 m in a square pattern.

2. The vacuum pumps efficiently combined with embankment surcharge and assisted by the field-distributed air–water separation tanks generated and maintained 80–90 kPa vacuum pressures at the sand blanket below the airtight membranes. The build-up pore pressures of − 50 to − 60 kPa were generated at -5 m elevation and

Table 4 Predicted settlements with 100 kPa surcharge during vac-PVD improvement

Layer depth		RR	CR	$\overline{\sigma}_{vo}$	$\Delta\overline{\sigma}_v$	$\Delta\overline{\sigma}_{vf}$	$\Delta\overline{\sigma}_{vm}$	ΔH
(m)				(kPa)	(kPa)	(kPa)	(kPa)	(m)
1.5	5	0.034	0.343	25	100	124	83	0.276
5	8	0.033	0.386	43	100	142	80	0.319
8	10	0.028	0.342	55	100	154	83	0.196
							Total	0.790

Table 5 Predicted settlements with 110 kPa surcharge during Vac-PVD improvement using designer's parameters

Layer depth		RR	CR	$\overline{\sigma}_{vo}$	$\Delta\overline{\sigma}_v$	$\Delta\overline{\sigma}_{vf}$	$\Delta\overline{\sigma}_{vm}$	ΔH
(m)				(kPa)	(kPa)	(kPa)	(kPa)	(m)
1.5	5	0.026	0.262	25	110	135	83	0.241
5	8	0.033	0.384	43	110	153	80	0.351
8	10	0.028	0.342	55	110	165	83	0.214
							Total	0.806

Table 6 Comparisons of observed and predicted final settlements and calculated consolidation degrees obtained from the Asaoka method, 1-D consolidation procedure, and pore water pressure data

Zone	Section	Observed	Asaoka		1-D consolidation		Pore water pressure data
		S_c	S_f	U	S_f	U	U
		(mm)	(mm)	(%)	(mm)	(%)	(%)
3	RA01	607	887	69	790	77	67
3	RB02	580	840	69	790	73	64
3	TA01	571	808	71	790	72	68

From Hansbo [1], the Asaoka's 1D consolidation equation and secondary compression settlement equation, c_h value can be derived as:

$$U_h = 1 - e^{\left(\frac{-8T_h}{F}\right)}$$

$$T_h = \frac{C_h t}{D_e^2}$$

$$S_t = S_f\left(1 - e^{\lambda t}\right)$$

$$S_s = hC'_{\alpha\varepsilon}\log\left(\frac{t}{t_p}\right)$$

$$S_n = \beta_0 + \beta_1 S_{n-1}$$

$$\beta_1 = \frac{1}{1 - \lambda\Delta t}$$

$$\beta_0 = f\beta_1$$

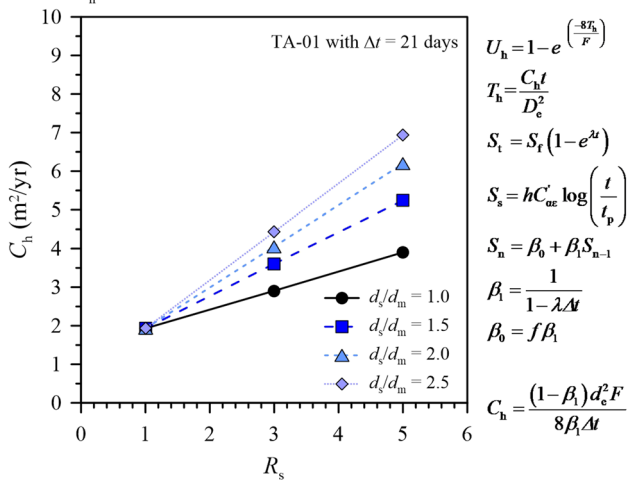$$C_h = \frac{(1 - \beta_1)d_e^2 F}{8\beta_1\Delta t}$$

Fig. 13 Back-calculated C_h values with $R_s = K_h/K_s$ for TA-01 at $\Delta t = 21$ days using the Asaoka method

slightly decreased with the depth ranging from − 40 to − 50 kPa at -10 m elevation.

3. The predicted ultimate consolidation settlements with 100 kPa vacuum pressure and surcharge load obtained from the Asaoka method (0.81 m) were slightly higher than the corresponding values derived by the 1-D consolidation method (0.79 m). The consolidation degrees from the 1-D consolidation method were marginally higher than the Asaoka method's corresponding values. The consolidation degree values from the pore pressures were lower than the Asaoka method.

4. After the first improvement, the average liquid limit values and water content were reduced to 100 and 80%, respectively. Moreover, the undrained shear strengths obtained from corrected field vane tests increased from 8–12 kPa to 20–27 kPa, and the maximum past pressures rose from 40–60 kPa to 78–118 kPa. By the current progress of the works, it is predicted that soft to medium stiff clay will be changed to medium stiff clay after the second improvement. The unit weights, undrained shear strengths, overconsolidation ratios, and maximum past pressures will be increased. However, water contents, void ratios, and compression indices will be further

Table 7 Prediction of the degree of consolidation using the Hansbo method at the time, $t = 5.3$ months (0.44 years)

PVD					Mandrel				Smear
Spacing	D_e	Width	Thickness	d_w	w_m	l_m	d_m		d_s
(mm)	(mm)	(mm)	(mm)	(mm)	(mm)	(mm)	(mm)		(mm)
1000	1130	100	4	52	120	60	96		191
	$D_e = 1.13s$			$d_w = \frac{a+b}{2}$			$d_m = \sqrt{\frac{4}{\pi} w_m l_m}$		$d_s = 2d_m$

$F_n = \ln(D_e/d_w) - 0.75$ $\quad F_n$ = additive effect due to PVD spacing

$F_s = (k_h/k_s - 1)\ln(d_s/d_w)$ $\quad F_s$ = additive effect due to smear effect

$F_s = \pi z(2L - z)k_h/q_w$ $\quad F_r$ = additive effect due to well resistance

$U_h = 1 - e^{-8T_h/F}$ $\quad$ The value of k_h/q_w is often smaller than 0.0001 for most practical cases. Thus, the value of well resistance, F_r, becomes negligible

$T_h = C_h t/D_e^2$

$F = F_n + F_s + F_r$

$U = 1 - (1 - U_h)(1 - U_v)$ $\quad$ For PVD improved zone, U_v can be neglected

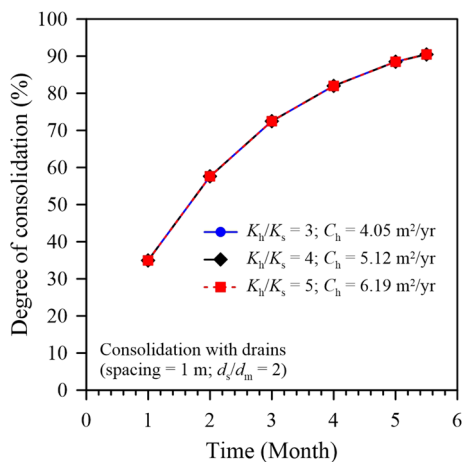| K_h/K_s	F_n	F_s	F_r	C_h (m²/year)	t (year)	D_e (m)	T_h	U_h (%)	U_v (%)	U (%)
3	2.33	2.61	4.94	4.05	0.44	1.13	1.401	90	0	90
4	2.33	3.91	6.24	5.12	0.44	1.13	1.771	90	0	90
5	2.33	5.21	7.51	6.19	0.44	1.13	2.141	90	0	90

Fig. 14 Degree of consolidation (DOC) with time using Hansbo method

reduced. Notably, the maximum past pressures should exceed 100 kPa.

5. From the Asaoka method, the back-calculated C_h value of 4 m²/year using $d_s/d_m = 2$, and $K_h/K_s = 3$ were obtained from the vacuum-PVD second improvement method. The K_h/K_s is slightly reduced due to the slight increase in Ks at the smear zone. Consequently, the C_h is also slightly increased. The corresponding values from the first improvement using PVD consisted of $d_s/d_m = 2$, $K_h/K_s = 5$, and $C_h = 3$ m²/year, similar to the previous project involving the adjacent runways at the Second Bangkok International Airport (SBIA). Thus, the K_h/K_s slightly decreased and C_h slightly increased

6. From inclinometer readings, maximum inward lateral displacements of 180 mm can be observed because of higher vacuum pressure than the embankment surcharge pressure. Ground cracks were located 6 m from the sealing membrane trench. The ground cracks illustrated that the vacuum pressure was more significant than the horizontal soil pressure, resulting in inward movement.

7. The vacuum-PVD second improvement with efficient field-distributed air–water separation system and airtight membranes with a connection of PVDs, horizontal prefabricated drains, and perforated pipes have been successfully applied in the runway extension project.

Fig. 15 Simplified soil profile and PVD zone of the vacuum-PVD improvement
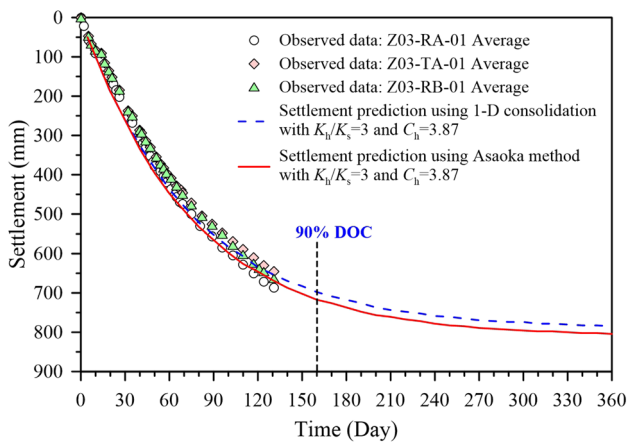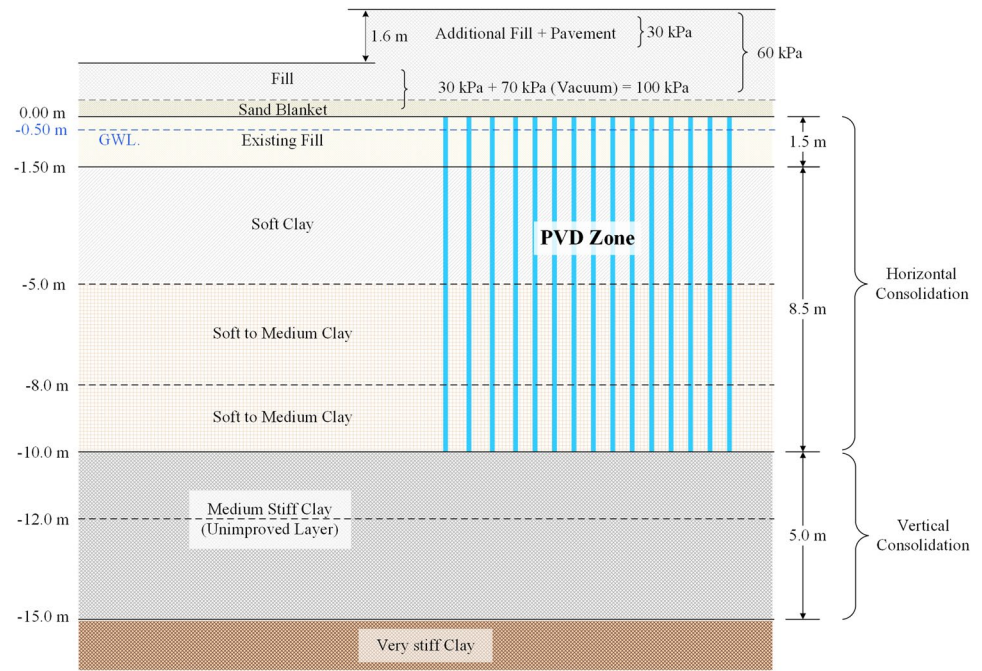

Fig. 16 Prediction of settlement with time using Asaoka method 1-D consolidation method
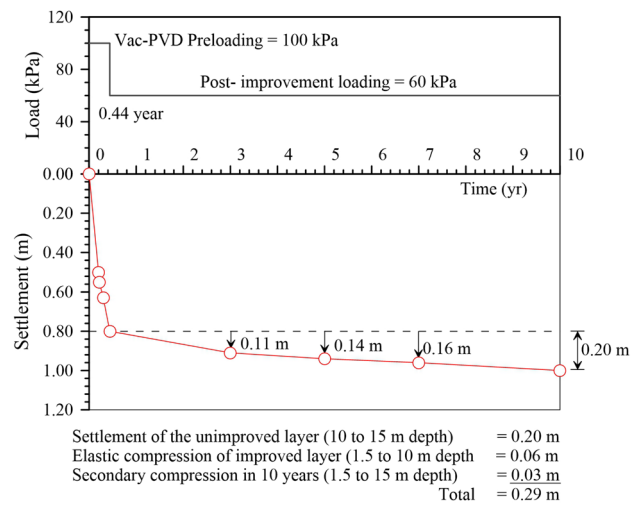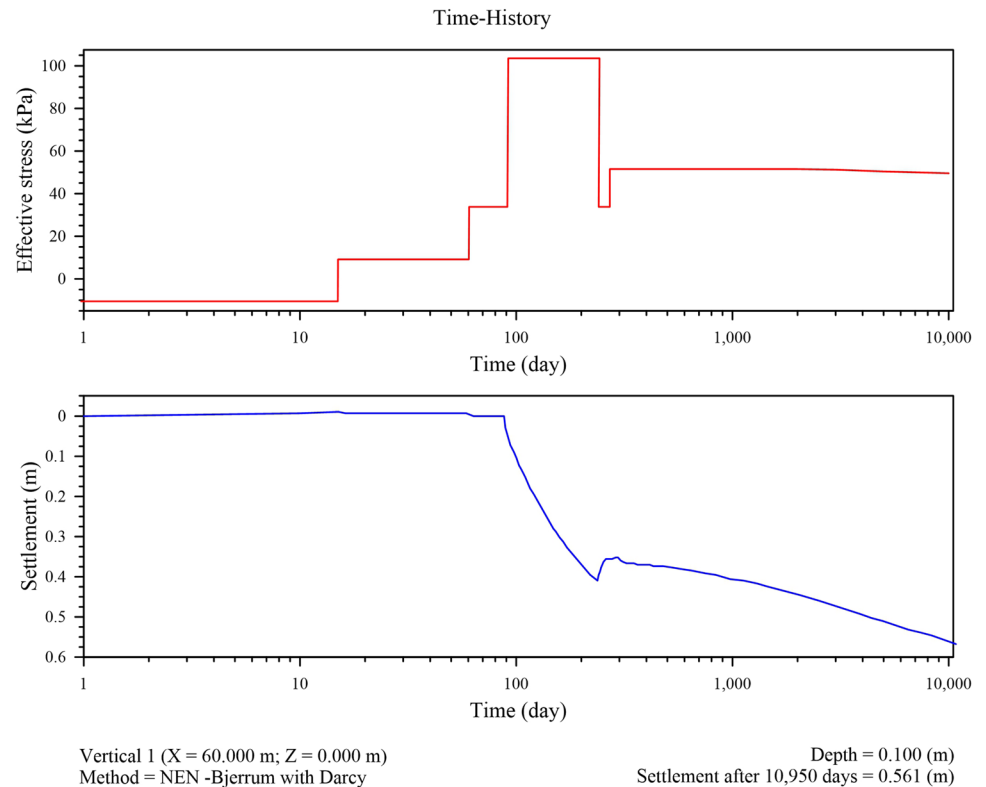

Fig. 17 Simplified prediction of 1-D consolidation settlement during vacuum-PVD improvement, including the calculated compressions during 10 years of post-improvement operation

Table 8 Predicted settlements with 60 kPa surcharge after vac-PVD improvement

Layer depth (m)		RR	CR	$\bar{\sigma}_{vo}$ (kPa)	$\Delta\bar{\sigma}_v$ (kPa)	$\Delta\bar{\sigma}_{vf}$ (kPa)	$\Delta\bar{\sigma}_{vm}$ (kPa)	ΔH (m)
1.5	5	0.054	0.262	25	60	85	115	0.005
5	8	0.069	0.355	43	60	103	120	0.022
8	10	0.069	0.305	55	60	115	120	0.035
10	12	0.031	0.324	65	60	125	92	0.096
12	15	0.041	0.289	80	60	140	110	0.108
							Total	0.265

Fig. 18 Predicted settlements during ground improvement and 30 years' operation by the design consultant of the runway extension project

Vertical 1 (X = 60.000 m; Z = 0.000 m)
Method = NEN -Bjerrum with Darcy

Depth = 0.100 (m)
Settlement after 10,950 days = 0.561 (m)

Declarations

References

1. Hansbo S (1979) Consolidation of clay by band-shaped prefabricated drains. Ground Eng 12(5):16–25
2. Hansbo S (1981) Consolidation of fine-grained soils by prefabricated drains. Proc Int Conf Soil Mech Found Eng 3:677–682
3. Bergado DT, Balasubramaniam AS, Fannin RJ, Holtz RD (2002) Prefabricated vertical drains (PVDs) in soft Bangkok clay: a case study of the new Bangkok International Airport project. Can Geotech J 39(2):304–315

4. Abuel-Naga H, Bergado DT, Gniel J (2015) Design chart for PVD improved ground. Geotext Geomembr 43:6

5. Deng Y, Kan ME, Indraratna B, Zhong R (2017) Finite element analysis of vacuum consolidation with modified compressibility and permeability parameters. Int J Geosynth Ground Eng 3(2):1–13

6. Koerner RM, Koerner MR, Koerner GR (2017) Utilizing PVDs to provide shear strength to saturated fine-grained foundation soils. Int J Geosynth Ground Eng 3(4):1–12

7. Khaimook P, Chai J (2019) Improving intermediate soils by vacuum consolidation–compaction technique. Int J Geosynth Ground Eng 5(2):1–9

8. Qi C, Li R, Gan F, Zhang W, Han H (2020) Measurement and simulation on consolidation behaviour of soft foundation improved with prefabricated vertical drains. Int J Geosynth Ground Eng 6(2):1–10

9. Badarinath R, El Naggar H (2021) Improving the stability of high embankments founded on soft marine clay by utilizing prefabricated vertical drains and controlling the pace of construction. Int J Geosynth Ground Eng 7(3):1–27

10. Bergado DT, Asakami H, Alfaro MC, Balasubramaniam AS (1991) Smear effects of vertical drains on soft Bangkok clay. J Geotech Eng ASCE 117(10):1509–1530

11. Abuel-Naga HM, Bouazza A (2009) Equivalent diameter of a prefabricated vertical drain. Geotext Geomembr 27:227–231

12. Kjellmann W. Consolidation of clay soil by means of atmospheric pressure. In: Proceedings on Soil Stabilization Conference, Boston, USA. 1952; 258–63.

13. Anda R, Fu HT, Wang J, Lei H, Hu X, Ye Q, Cai Y, Xie Z (2020) Effects of pressuring timing on air booster vacuum consolidation of dredged slurry. Geotext Geomembr 48:491–503

14. Cai YQ, Xie ZW, Wang J, Wang P, Geng XY (2018) New approach of vacuum preloading with booster PVDs to improve deep marine strata. Can Geotech J 55(10):1359–1371

15. Chai JC, Carter JP, Hayashi S (2006) Vacuum consolidation and its combination with embankment loading. Can Geotech J 43(10):985–996

16. Chai JC, Miura N, Bergado DT (2008) Preloading clayey deposit by vacuum pressure with cap-drain: analyses versus performance. Geotext Geomembr 26:220–230

17. Chai JC, Ong CY, Carter JP, Bergado DT (2013) Lateral displacement under combined vacuum pressure and embankment loading. Geotechnique 63(10):842–856

18. Chai JC, Lu Y, Fu H (2019) Groundwater level under vacuum consolidation. Proc Inst Civil Eng Ground Improv 174(2):1–7

19. Chai JC, Fu HT, Wang J, Shen SL (2020) Behavior of a PVD unit cell under vacuum pressure and a new method for consolidation analysis. Comput Geotech 120:103415

20. Chu J, Yan SW, Yang H (2000) Soil improvement by the vacuum preloading method for an oil storage station. Geotechnique 50(6):625–632

21. Fang Y, Gou L, Huang J (2019) Mechanical test on inhomogeneity of dredged fill during vacuum preloading consolidation. Mar Resour Geotech 37(8):1007–1017

22. Hayashi H, Hatakeyama O, Hashimoto H (2019) Reducing the secondary consolidation of peat ground using vacuum consolidation. Proc Inst Civ Eng Ground Improv 174(3):1–12

23. Indraratna B, Rujikiatkamjorn C, Sathananthan I (2005) Analytical and numerical solutions for a single vertical drain including the effects of vacuum preloading. Can Geotech 42:994–1014

24. Indraratna B, Geng XY, Rujikiatkamjorn C (2010) Review of methods of analysis for the use of vacuum preloading and vertical drains for soft clay improvement. Geomech Geoeng 5(4):223–236

25. Indraratna B, Rujikiatkamjorn C, Balasubramaniam AS, McIntosh G (2012) Soft ground improvement via vertical drains and vacuum assisted preloading. Geotext Geomembr 30:16–23

26. Lam LG, Bergado DT, Hino T (2015) PVD improvement of soft Bangkok clay with and without vacuum preloading using analytical and numerical analyses. Geotext Geomembr 43(6):547–557

27. Lei HY, Hu Y, Zheng G, Liu JJ, Wang L, Liu YN (2019) Improved air booster vacuum preloading method for newly dreged fills: laboratory model study. Mar Georesour Geotech 38(4):493–510

28. Long PV, Bergado DT, Nguyen LV, Balasubramaniam AS (2013) Design and performance of soft clay improvement using PVD with and without vacuum consolidation. Geotech Eng J SEAGS AGSSEA 44(4):37–52

29. Long PV, Nguyen LV, Bergado DT, Balasubramaniam AS (2015) Performance of PVD improved soft ground using vacuum consolidation methods with and without airtight membrane. Geotext Geomembr 43:473–483

30. Long PV, Nguyen LV, Tri TD, Balasubramaniam AS (2016) Performance and analyses of thick soft clay deposit improved by PVD with surcharge preloading and vacuum consolidation—a case study at CMIT. Geotech Eng J SEAGS AGSSEA 47:1–10

31. Ni P, Xu K, Mei J, Zhao Y (2019) Effect of vacuum removal on consolidation settlement under a combined vacuum and surcharge preloading. Geotext Geomembr 47:12–22

32. Saowapakpiboon J, Bergado DT, Thann YM, Voottipruex P (2009) Assessing the performance of PVD with vacuum and heat preloading. Geosynth Int 16(5):384–392

33. Saowapakpiboon J, Bergado DT, Youwai S, Chai JC, Wanthong P, Voottipruex P (2010) Measured and predicted performance of prefabricated vertical drains (PVDs) with and without vacuum preloading. Geotext Geomembr 28:1–11

34. Saowapakpiboon J, Bergado DT, Voottipruex P, Lam LG, Nakakuma K (2010) PVD improvement combined with surcharge and vacuum preloading including simulations. Geotext Geomembr 29(1):74–82

35. Wang J, Fang ZQ, Cai YQ, Chai JC, Wang P, Geng XY (2018) Preloading using fill surcharge and prefabricated vertical drains for an airport. Geotext Geomembr 46(5):575–585

36. Wang P, Yu F, Zhou Y, Wang J (2019) Effect of a sealed connector on the improvement of dredged slurry under vacuum preloading. Proc Inst Civ Eng Geotech Eng 173(3):1–8

37. Yan SW, Feng XW, Chu J (2009) Mechanism of using vacuum preloading method in improving soft clay layers. Advances in ground improvement: research to practice in the United States and China. ASCE, North America, pp 308–317

38. Zhang D, Fu H, Wang J, Zhu D, Hu D, Hu X, Du Y, Gou C, Wang C, Li M, Wu H (2020) Behaviour of thick marine deposits subjected to vacuum combined with surcharge preloading. Mar Resour Geotechnol. https://doi.org/10.1080/1064119x.2020.1817204

39. Deng YF, Liu L, Cui YJ, Feng Q, Chen XL, He N (2018) Colloid effect on clogging mechanism of hydraulic reclamation mud improved by vacuum preloading. Can Geotech J 56(5):611–620

40. Wang P, Han Y, Zhou Y (2020) Apparent clogging effect in vacuum-induced consolidation of dredged soil with prefabricated vertical drains (PVDs). Geotext Geomembr. https://doi.org/10.1016/j.geotexmem.2020.02.010

41. Xu BH, He N, Jiang YB, Zhou YZ, Zhan XJ (2020) Experimental study on the clogging effect of dredged fill surrounding the PVD under vacuum preloading. Geotext Geomembr 48(5):614–624

42. Zhou Y, Wang P, Shi L, Cai Y, Wang J (2021) Analytical solution on vacuum consolidation of dredged skurry considering clogging effects. Geotext Geomembr 49(3):842–851

43. Seah TH, Tangghansup B, Wongsatian P (2004) Horizontal coefficient of consolidation of soft Bangkok clay. Geotech Test J ASTM 27(5):430–440

44. Balasubramaniam AS, Bergado DT, Phienwej N. The Full Scale Field Test of Prefabricated Vertical Drains for The Second

Bangkok International Airport (SBIA), Final Report, Div. of Geotech. and Trans. Eng. AIT, Bangkok, Thailand. 1995.

45. Bergado DT, Chaiyaput S, Artidteang S, Nguyen NT (2020) Microstructures within and outside the smear zones for soft clay improvement using PVD only, vacuum-PVD, thermo-PVD and thermo-vacuum-PVD. Geotext Geomembr 48(6):828–843

46. Bergado DT, Chai JC, Miura N, Balasubramaniam AS (1998) PVD improvement of soft Bangkok clay with combined vacuum and reduced sand embankment preloading. Geotech Eng 29(1):95–121

47. Chai JC, Carter JP, Hayashi S (2005) Ground deformation induced by vacuum consolidation. J Geotech Geoenviron Eng 131(12):1552–1561

48. Zhou Y, Chai JC (2017) Equivalent 'smear' effect due to non-uniform consolidation surrounding a PVD. Geotechnique 67(5):410–419

49. ASTM D4751–20b (2020) Standard test method for determining apparent opening size of a geotextile. ASTM International, West Conshohocken

50. ASTM D4632, D4632M-15a (2015) Standard test method for grab breaking load and elongation of geotextiles. ASTM International, West Conshohocken

51. ASTM D4595–17 (2017) Standard test method for tensile properties of geotextiles by the wide-width strip method. ASTM International, West Conshohocken

52. ASTM D4833, D4833M-07 (2020) Standard test method for index puncture resistance of geotextiles, geomembranes and related products. ASTM International, West Conshohocken

53. ASTM D4716, D4716M-20 (2020) Standard test method for determining the (in-plane) flow rate per unit width and hydraulic transmissivity of a geosynthetic using a constant head. ASTM International, West Conshohocken

54. Bergado DT, Manivannan R, Balasubramaniam AS (1996) Filtration criteria for prefabricated vertical drain geotextile filter jackets in soft Bangkok clay. Geosynth Int 3(1):63–83

55. Miura N, Chai JC, Yoyota K. Investigation of some factors affecting discharge capacity of PVD. In: Proceedings of 6th International Conference in Geosynthetics. Atlanta, USA. 1998; 845–850.

56. Bergado DT, Manivannan R, Balasubramaniam AS (1996) Proposed criteria for discharge capacity of prefabricated vertical drains. Geotext Geomembr 14:481–505

57. Bergado DT, Long PV, Balasubramaniam AS (1996) Compressibility and flow parameters from PVD improved soft bangkok clay. Geotech Eng J 27(1):1–20

58. Hansbo S. Design aspects of vertical drains and lime column installation. In: Proceedings 9th Southeast Asian Geotechnical Conference. 1987; 2(8):1–12

59. Indraratna B, Redana IW (1998) Laboratory determination of smear zone due to vertical drain installation. J Geotech Eng 125(1):96–99

60. Bergado DT, Enriquez AS, Sampaco CL, Alfaro MC, Balasubramaniam AS (1992) Inverse analysis of geotechnical parameters on improved soft bangkok clay. J Geotech Eng 118(7):1012–1030

61. Carrillo N (1942) Simple two- and tree-dimensional cases in the theory of consolidation of soils. J Math Phys 21:1–5

62. Long PV, Bergado DT, Giao PH, Balasubramaniam AS, Quang NC. Back Analyses of compressibility and flow parameters of PVD improved soft ground in Southern Vietnam. In: Proceedings of the 8th International Conference on Geosynthetics, Yokohama. 2006; 2:465–68.

63. Asaoka A (1978) Observational procedure of settlement prediction. Soil Found 18(4):87–101

64. Wu J, Xuan Y, Deng Y, Li X, Zha F, Zhou A (2020) Combined vacuum and surcharge preloading method to improve Lianyungang soft marine clay for embankment widening project: a case. Geotext Geomembr 49(2):452–465

65. Chu J, Yan SW (2005) Estimation of degree of consolidation for vacuum preloading projects. Int J of Geosynth Ground Eng 5(2):158–165

66. Artidteang S, Bergado DT, Saowapakpiboon J, Teerachaikulpanich N, Kumar A (2011) Enhancement of efficiency of prefabricated vertical drains using surcharge vacuum and heat preloading. Geosynth Int 18(1):35–47

67. Bergado DT, Jamsawang P, Jongpradist P, Likitlersuang S, Pantaeng C, Kovittayanun N, Baez F (2021) Case study and numerical simulation of PVD improved soft Bangkok clay with surcharge and vacuum preloading using a modified air-water separation system. Geotext Geomembr. https://doi.org/10.1016/j.geotexmem.2021.09.009